

RANGE OF VALIDITY OF A MODIFIED K-EPSILON MODEL OF THE NON-REACTING FLOW FROM A PRECESSING JET NOZZLE

Elizabeth J. SMITH, Graham J. NATHAN and Bassam B. DALLY

School of Mechanical Engineering, The University of Adelaide, Adelaide SA 5005, AUSTRALIA

ABSTRACT

One method for improving combustion within rotary kilns is the use of the Precessing Jet (PJ) nozzle. The flow emerging from a PJ nozzle is 3-D and highly unsteady, resulting in initial rates of spread and decay that are much greater than those of simple jet flows. Modelling the entire flow using a 3-D, time dependent model would not usually be justified as an industrial design tool. Instead we have sought to develop a CFD model which simulates the effect of precession on the mean spread and decay rates of a jet. A robust and relatively simple turbulence model, the two-equation $k-\epsilon$ model, is used. Assuming symmetry and using a 2-D approximation further simplifies the model. This paper assesses the robustness and range of validity of this numerical technique. The model is compared with experimental results for varying initial conditions, including effects of confinement, co-flow ratio, Reynolds number and nozzle configuration.

NOMENCLATURE

$C_{\epsilon 1}$	Dissipation rate equation production constant
$C_{\epsilon 2}$	Dissipation rate equation dissipation constant
C_{rms}	Centreline RMS concentration
C_{ja}	Jet axis concentration
D	PJ nozzle diameter
d	PJ nozzle inlet diameter
D_{duct}	Outer duct diameter
L	PJ nozzle length
Re	Reynolds number
U_c	Co-flow velocity
U_{ja}, U	Jet axis velocity
U_{je}	Jet exit velocity
x	Axial distance

INTRODUCTION

Rotary kilns, used in the production of cement clinker, alumina, lime and nickel, require high heat energy with product temperatures up to 1500°C. This is usually supplied by the combustion of fossil fuels. One method for reducing the NOx emissions and improving overall combustion within rotary kilns firing either gas or solid fuels (Nathan and Hill, 2002) is the use of the precessing jet technology developed at the University of Adelaide (Nathan et al., 1998).

Jet precession can be generated by a naturally occurring instability within an axisymmetric chamber downstream from a large sudden expansion. A schematic diagram of the precessing jet nozzle is shown in Figure 1. Flow enters the precessing jet (PJ) chamber through a large sudden expansion (Nathan et al., 1998, Kelso, 2001 and

Wong et al., 2002). The jet flow deflects asymmetrically to the wall of the chamber, where it reattaches. An unstable pressure field is created in the nozzle chamber causing the attached flow to precess azimuthally as it travels through the nozzle. On exiting the chamber the jet flow is deflected by a small lip and leaves at an angle of 40-60° to the nozzle geometric axis.

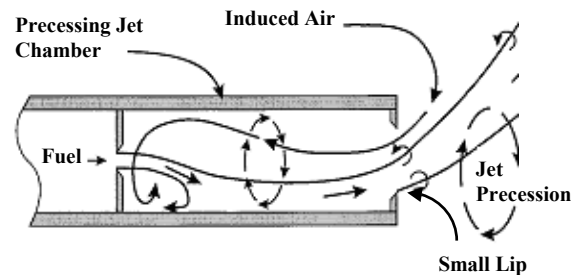


Figure 1: A schematic diagram of a precessing jet nozzle and flow (Parham, 1998).

The precessing jet has been successfully applied to rotary kilns producing cement clinker, alumina, lime and zinc oxide (Manias et al., 1996 and Rapson et al., 1995) and is licensed for use within these industries as the Gyro-Therm™ (Luxton et al., 1991) burner. When firing natural gas in rotary kilns, a precessing jet provides a more luminous flame, lower peak temperatures, high flame stability and about a 40% reduction in NOx emissions than comparable swirling and non-swirling flames.

The internal and initial emerging flow from a precessing jet nozzle is highly 3-D and unsteady. Its initial rates of spreading and decay are much greater than those of simple jet flows. However most of the combustion occurs downstream from this complex region (Newbold, 1997) where the unsteadiness in the flow is comparable with that in a simple jet. The extent of the rapid initial spread and decay is limited to an axial distance of approximately $x/D < 1.4$, where D is the diameter of the PJ chamber (Parham, 2000). The decay rate then decreases to a value more similar to that of the simple jet.

The region of flow where the decay rate dramatically changes can be characterised by an elbow point in the mean centre-line decay (Figure 2). The region upstream from the elbow point is referred to as the near field and is where true precession occurs. The region immediately downstream from the elbow point is referred to as the transitional region, describing the transition from precession dominated flow to flow more similar to that of the simple jet. The region downstream from $x/D > 4$ is

considered as the ‘far’ field where self similarity of the mean flow is approximated. True self-similarity of the flow does not occur until much further downstream in a free jet, and may never be achieved in a confined jet (Richards and Pitts, 1993).

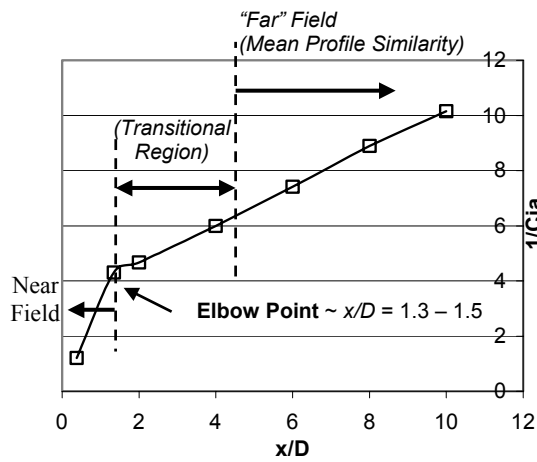


Figure 2: Plot of normalised jet concentration (C_{ja}) axial decay depicting the three dominant regions of the emerging PJ flow, where nozzle diameter $D=38\text{mm}$ (Parham, 2000 & Smith et al., 2003).

To further the application of PJ flows in industry, improved predictive capability is desired. A CFD model offers the potential for prediction of heat transfer and pollutant emissions. Preliminary work by Smith et al. (2003) established a simplified 2-D CFD based technique to simulate the effect of precession on the mean spread and decay rates. This modelling technique will be applied to capture flow, mixing and reactive fields in PJ flames.

The approach taken in this project was to decouple the reacting and heat release from the flow and mixing fields by modelling isothermal flows. Subsequent stages will involve the introduction of a simple combustion model along with radiation, soot formation and NO_x production models and the use of particles.

In this paper we report on the robustness of this model to variations in initial conditions such as, confinement, co-flow ratio, Reynolds number and nozzle configuration. Direct comparison is made with experimental measurements for mean and RMS concentration decay and mean velocity decay.

MODELLING APPROACH

It is known that the k- ϵ model over-predicts the spreading and decay rate of a round jet flow by 40% (Pope, 1978). To improve the accuracy of the k- ϵ model for solving round jet flows the turbulence constants ($C_{\epsilon 1}$ and $C_{\epsilon 2}$) of the dissipation term may be modified, as they are responsible for the generation/destruction of the energy dissipation. Modifications to the turbulence constants have been suggested in the past by McGuirk and Rodi (1979), Morse (1977), Launder et al. (1972), and Pope (1978). All modifications involve the turbulence constants becoming functions of the velocity decay rate and jet width. For self-similar round jets it was found that modifications made by Morse (1977) and Pope (1978) lead to $C_{\epsilon 1}$ having a fixed value of 1.6. To examine the impact of the modifications to the accuracy of the k- ϵ

model when used for round jets, Dally et al. (1998) compared the use of modifications made by Morse (1977) and Pope (1978) with the standard k- ϵ constants ($C_{\epsilon 1}=1.44$ and $C_{\epsilon 2}=1.92$) and a fixed value for $C_{\epsilon 1}=1.6$ with $C_{\epsilon 2}=1.92$. It was found that the modifications by Morse and Pope did improve the accuracy of the k- ϵ model when compared to the standard k- ϵ constants. However the fixed value of $C_{\epsilon 1}=1.6$ with $C_{\epsilon 2}=1.92$ matched the experimental results the closest.

In previous work by Smith et al. (2003) it was shown that, as the ratio of $C_{\epsilon 1}/C_{\epsilon 2}$ is increased, the spreading rate of a round jet decreases, suggesting an inverse relationship. The spreading rate was found to depend not only on the ratio of $C_{\epsilon 1}/C_{\epsilon 2}$ but also the value of $C_{\epsilon 1}$. As the value of $C_{\epsilon 1}$ is increased, the decay rate decreases, producing a longer narrower flow.

This technique of varying the turbulence constants to alter the spreading and decay rate of a round simple jet may be applied to the analysis of the precessing jet flow. That is, $C_{\epsilon 1}$ and $C_{\epsilon 2}$ can be varied to seek to match the measured spreading and decay rates of the precessing jet flow.

The commercially available CFD program CFX 4.4 is used for all calculations. CFX uses a finite volume formulation over a structured mesh. The CFX program is commonly used throughout industry and accommodates user routines to enable changes to the default settings to be made. Further information regarding the modelling technique is provided by Smith et al. (2003).

CONFIGURATION AND INITIAL CONDITIONS

The computational domain for the precessing jet models extends 20 diameters upstream from the inlet of the nozzle to ensure fully developed pipe flow, and 1 metre downstream from the exit of the nozzle to ensure capture of data in the self-similar region. A schematic diagram of the computational domain is shown in Figure 3. Grid cells were placed closer together near to the jet walls and further apart with increasing distance from the jet exit. Grid independence is ensured for all geometries.

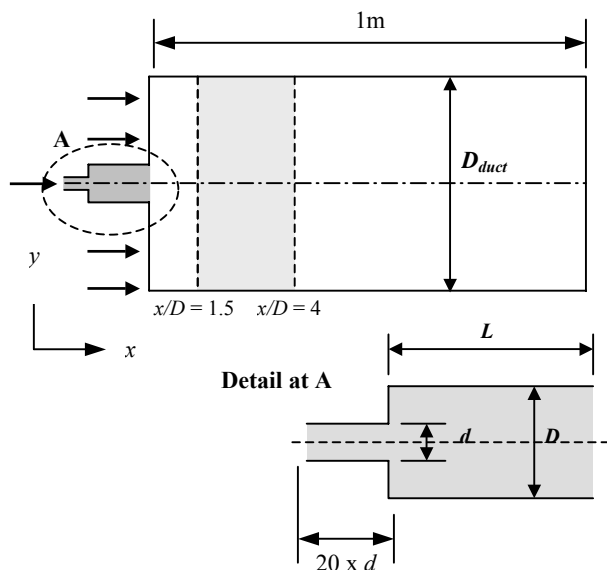


Figure 3: Schematic diagram of the computational domain

The k- ϵ turbulence model is applied with Hybrid differencing for all equations. Convergence was considered to be complete when the ratio of mass residuals to mass entering the jet was less than 1×10^{-6} . The flow is assumed to be non-reacting and steady state. A “Mixed is Burnt” subroutine is used to extract the conserved scalar data, mean and RMS mixture fraction. Temperature is under-relaxed to prevent heat release and remains constant at 293K. Assuming symmetry and using a two-dimensional (2-D) approximation further simplifies the model. Three different precessing jet configurations were examined with varying initial conditions. A summary of these conditions is provided in Table 1.

D	U_c/U_{je}	D_{duct}/D	Re
Effect of Confinement, medium: water			
38mm	0.055	10.3	20,000
38mm	0.055	7.6	20,000
38mm	0.055	12.9	20,000
Effect of Co-flow ratio, medium: water			
38mm	0.055	10.3	66,100
38mm	0.034	10.3	66,100
38mm	0.098	10.3	66,100
38mm	0.147	10.3	66,100
38mm	0.196	10.3	66,100
Effect of nozzle Configuration, medium: water			
38mm	0.055	10.3	20,000
10mm	0.055	10.3	20,000
25mm	0.055	10.3	20,000
Effect Reynolds number, medium: water			
38mm	0.055	10.3	20,000
38mm	0.055	10.3	66,100
38mm	0.055	10.3	200,000

Table 1: Summary of initial conditions

PRELIMINARY ANALYSIS

To match both the near and far fields of the PJ flow different constants are required for different regions. The computational domain is split into six regions (Figure 4), that of the inlet jet (Region I), PJ nozzle (Region II), near field (Region IV), transitional field (Region V), far field (Region VI) and co-flow (Region III). The non-shaded regions are configured with the modified constants (MSJ-1, where $C_{\epsilon 1} = 1.6$ and $C_{\epsilon 2} = 1.92$, Dally et al., 1998) and the regions shaded in grey are configured to provide modified decay rates within these regions. The constants within Region II are configured for the PJ nozzle to provide an appropriate velocity profile at the PJ nozzle exit. Constants within Region IV are configured for the near field to provide appropriate high initial decay rate while the constants in Region VI are configured to provide the dramatic step change in decay rates between the near and far fields. This model is referred to as the six-zone model (PJ6Z-1: PJ model 6 Zones Version 1). The switching between constants within the defined regions is achieved by using a “User Routine” within CFX.

The experimental data chosen for the purpose of initially calibrating the six zone PJ model was obtained using Planar laser Induced Fluorescence in a water tunnel test facility located in the Department of Mechanical Engineering at The University of Adelaide (Parham, 2000). These measurements provide extensive mean and RMS concentration data in non-reacting conditions. The initial conditions for this PJ are: $D = 38\text{mm}$, $U_c/U_{je} = 0.055$, $Re = 66,100$ and $D_{duct}/D = 10.3$.

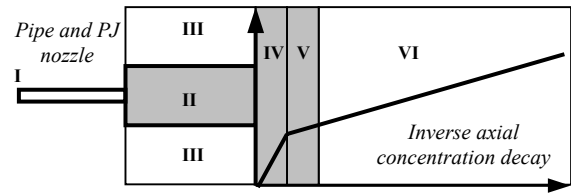
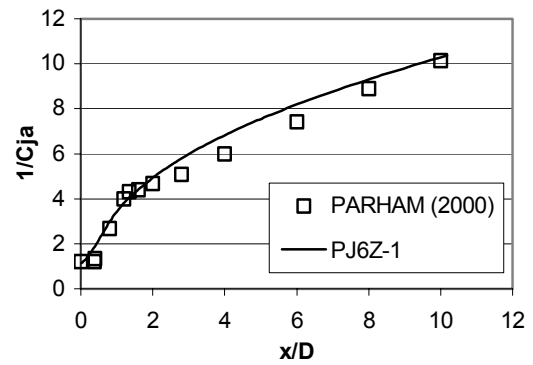
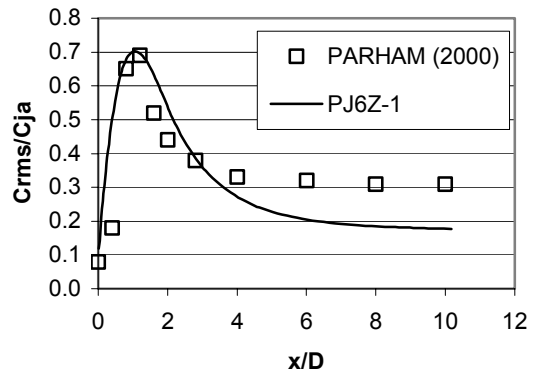


Figure 4: The six computational regions used to model the precessing jet flow field. (Smith et al., 2003).

The calibrated model matches the near and far field decay rates for both mean and RMS data reasonably well (Figure 5). The model provides a good match of the distinctive peak for RMS decay, however the downstream asymptotic value has been underestimated. It is known that the experimental results collected by Parham (2000) have also slightly underestimated the RMS concentration. This is due to the inability of a planar imaging technique to resolve the Batchelor scale in turbulent conditions with water as the working fluid.



a. Mean concentration Decay



b. RMS concentration Decay

Figure 5: Plot of mean (a) and RMS (b) axial concentration decay comparing the six zone precessing jet model (PJ6Z-1) with measured data for the precessing jet (Parham, 2000), where $D = 38\text{mm}$. (Smith et al., 2003).

Preliminary measurements of the non-reacting velocity decay for the precessing jet were collected by Nobes et al. (1998). The measurements were performed in air using PIV. The data contains mean and RMS velocity measurements for two PJ nozzles, $D = 10\text{mm}$ and $D = 25\text{mm}$, with $D_{duct}/D = 10.3$. Both jets had $U_c/U_{je} = 0.055$ and $Re = 20,000$. The data was published in an internal report (Nobes et al., 1998) and provides a useful preliminary comparison for the numerical model. Figure 6 compares

the numerical and experimental velocity decay for precessing jets with $D = 10\text{mm}$ and 25mm . The model has predicted the high initial decay rate of the emerging flow as well as the significantly reduced decay rate in the far field. However a core region for $x/D < 0.5$ is evident in the experiment which was not captured in the calculations. It is deduced that this discrepancy arises from a fundamental limitation in modelling an unsteady flow with a steady state model. Unlike the scalar field, the near field time-averaged velocity is not bell shaped, but exhibits a double peak (Wong et al., 2002). Hence the near-field time averaged velocity and scalar fields are inherently dis-similar in this region. However, since very little combustion occurs in this region, this approximation may not be significant in the overall performance of the flame.

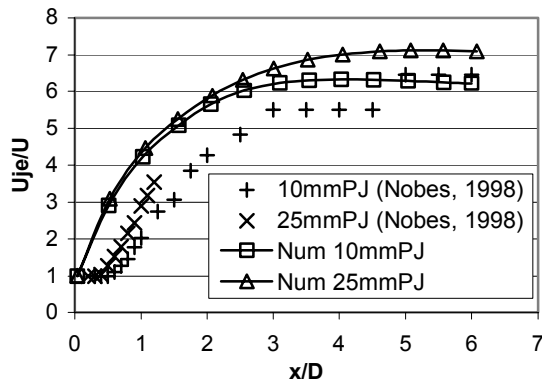


Figure 6: Plot of axial mean velocity decay comparing the numerical model with experimental data for the $D = 25\text{mm}$ PJ and $D = 10\text{mm}$ PJ (Nobes, 1998).

RESULTS

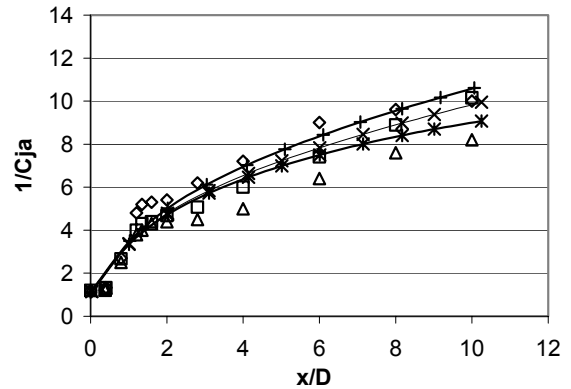
Effect of Varying Confinement

The six zone precessing jet model (PJ6Z-1) developed by Smith et al. (2003) was calibrated to match the spread and decay rates of the $D = 38\text{mm}$ PJ emerging into a confinement of $D_{duct}/D = 10.3$. This model is now applied to two additional duct confinement ratios, $D_{duct}/D = 7.6$ and 12.9 . The effect of confinement on the mean and RMS concentration decay rates is presented in Figure 7. The co-flow to jet velocity ratio is $U_c/U_{je} = 0.055$ for each confinement.

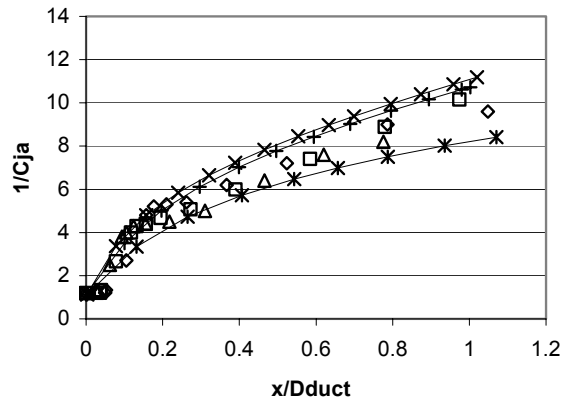
The measurements of Parham (2000) indicate that, as the ratio of duct to PJ nozzle diameter increases, the inverse jet concentration decay is shifted downwards. This is predicted by the numerical model for the $D_{duct}/D = 10.3$ and 12.9 cases. However the confinement ratio of $D_{duct}/D = 7.6$ produces a profile that is much lower than expected (Figure 7a). It should be located above the profile for $D_{duct}/D = 10.3$. This suggests that the constants under predict the decay rate for highly confined flows with confinement ratios below $D_{duct}/D = 8$.

Parham (2000) has shown that the duct diameter is better at normalising the axial distance than the nozzle diameter, and the effect of the $D_{duct}/D = 7.6$ confinement on the model is more evident when plotted in this format (Figure 7b). All of the inverse concentration profiles should collapse onto the one profile, like the profiles for $D_{duct}/D = 10.3$ and 12.9 . However the $D_{duct}/D = 7.6$ profile is situated much lower than these two profiles.

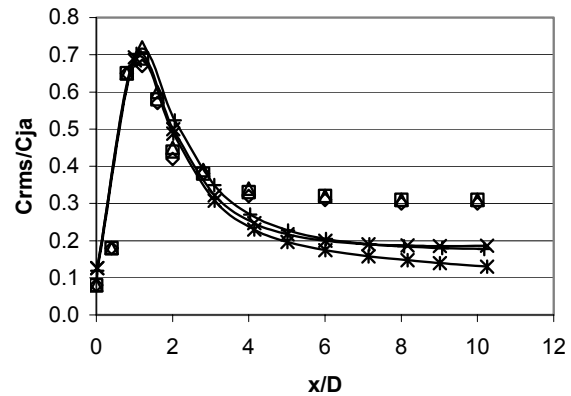
The effect of confinement ratio on the concentration fluctuation intensity was shown to be negligible, and that the location of the distinctive peak and downstream asymptote remained the same for all confinement ratios (Figure 7c).



a. Mean concentration Decay, x-axis normalised to x/D



b. Mean concentration Decay, x-axis normalised to x/D_{duct}



c. RMS concentration Decay, x-axis normalised to x/D

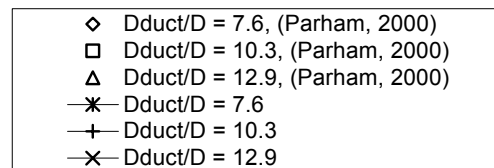


Figure 7: Plot of axial mean (a & b) and RMS (c) concentration decay comparing the effect of confinement on the calibrated model.

Effect of Varying Co-flow Velocity Ratio

Experimental measurements collected by Parham, 2000, indicate that, as the co-flow velocity ratio, U_c/U_{je} , is varied, there is little change in the inverse concentration decay in the near field or far field. However, the magnitude of the inverse concentration is shifted higher as the velocity ratio increases, so that at a given axial location the value of the inverse concentration increases with increasing co-flow velocity (Parham, 2000). This trend is reproduced by the numerical model. The effects of co-flow velocity ratio on the mean and RMS concentration decay can be seen in Figure 8. Experimental and numerical data have been plotted for the two extreme cases of co-flow velocity ratios, that is, $U_c/U_{je} = 0.034$ and 0.196 .

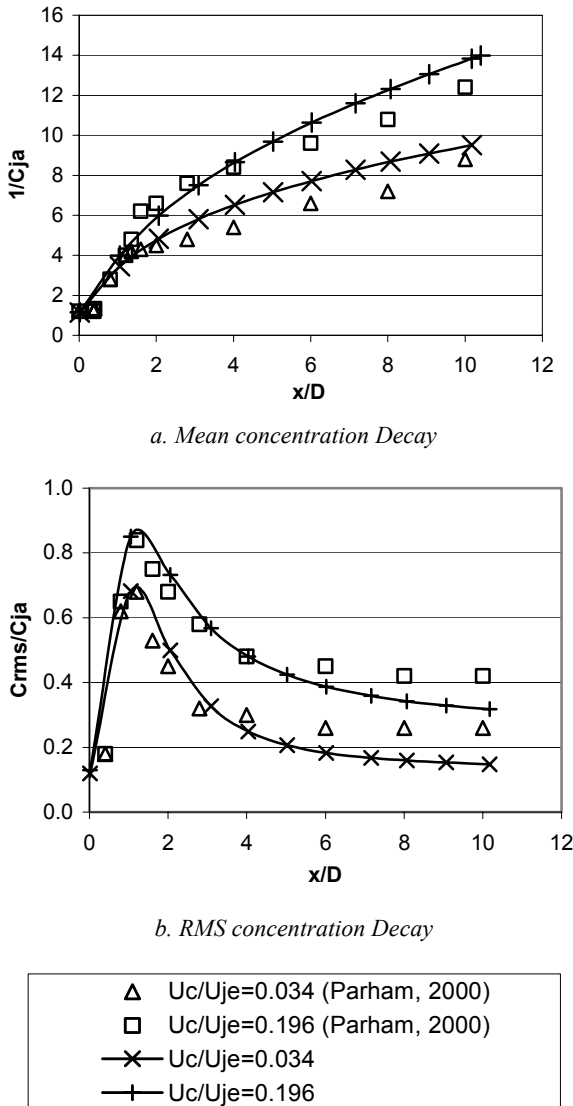


Figure 8: Plot of axial mean (a) and RMS (b) concentration decay comparing the calibrated model with two variations in co-flow ratio.

Results for numerical and experimental RMS concentration decay are summarised in Table 2. As the ratio of co-flow to jet velocity increases, the maximum value of the distinctive peak also increases and the breadth of the peak is stretched in an axial direction with

increasing co-flow velocity (Parham, 2000). However the location of the peak does not change. The asymptotic value of the fluctuation intensity in the far field also increases. The numerical model has predicted the distinctive peak of the RMS decay reasonably well. However the asymptotic value of the fluctuation intensity has been underestimated by 30% on average. It should be noted that the RMS data measured by Parham (2000) have also been underestimated.

U_c/U_{je}	C_{rms}/C_{ja} Peak		C_{rms}/C_{ja} $x/D > 10$	
	Num.	Exp.	Num.	Exp.
0.034	0.70	0.69	0.15	0.26
0.055	0.70	0.70	0.18	0.30
0.098	0.77	0.75	0.24	0.35
0.147	0.82	0.82	0.28	0.38
0.196	0.85	0.84	0.32	0.43

Table 2: Comparison of RMS concentration decay between numerical and experimental (Parham, 2000) data.

Effect of Varying Nozzle Configuration

Although experimental data is only available for one PJ nozzle configuration ($D = 38\text{mm}$), it is known that the spread and decay rates of precessing jets are relatively insensitive to nozzle size. Figure 9 shows that there is little variation in predicted spread and decay rate for all configurations, illustrating that the model is independent of nozzle size. Where $D_{duct}/D = 10.3$ and $U_c/U_{je} = 0.055$.

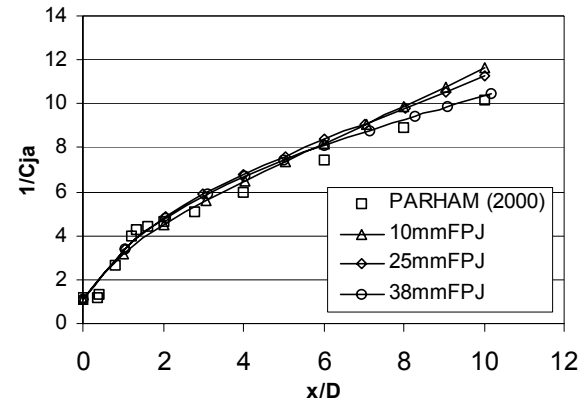


Figure 9: Plot of axial mean concentration decay comparing experimental data (Parham, 2000) with the calibrated model for three PJ configurations.

Effect of Varying Reynolds Number

To determine the model's sensitivity to variation in velocity, three Reynolds numbers were compared. Unfortunately experimental measurements for mean axial concentration decay are only available for one Reynolds number, $Re = 66,100$. Figure 10 shows the effect of Reynolds number on the axial mean mixture fraction for PJ nozzle $D = 38\text{mm}$ with $Re = 20,000$, $66,100$ and $200,000$, where $D_{duct}/D = 10.3$ and $U_c/U_{je} = 0.055$.

There is little variation in decay rate between the three values and hence the model is considered to be independent of Reynolds number within this range.

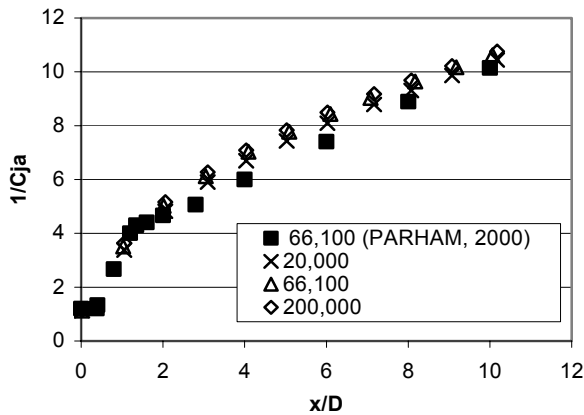


Figure 10: Plot of axial mean concentration decay comparing experimental data (Parham, 2000) with the calibrated model for three Reynolds numbers.

CONCLUSION

This study has assessed the robustness of the six zone precessing jet model developed in previous work by Smith et al. (2003). For varying co-flow and confinement ratios the model has reproduced the trends found experimentally. It was found that, as the co-flow velocity is increased, the profile for inverse concentration decay is also increased. When the confinement ratio of the emerging PJ flow is increased, the profile of the inverse concentration decay is reduced. However this study has shown that the model is sensitive to highly confined conditions, but only within a range not usually found in practice. Three PJ configurations and Reynolds numbers were compared and there was little difference in their resulting inverse concentration profiles, showing that the model is independent of both PJ size and Reynolds number.

The preliminary velocity comparison has shown that the PJ model does not reproduce the initial core region. This is deduced to be a fundamental limitation in the use of a steady state model for an unsteady flow, since the real velocity and scalar fields are not similar. However the combustion calculations are based on the scalar field so this discrepancy may not effect the predictions too greatly. This assessment is deemed to justify extension of the model to evaluate its usefulness in prediction of NOx emissions and heat transfer characteristics.

Currently this model is being extended to reacting flows where flame length, heat flux and NOx emissions are of prime interest.

ACKNOWLEDGEMENTS

The authors wish to thank the ARC SPIRT scheme, the Sugar Research Industry (SRI) and Fuel and Combustion Technology (FCT) for their support of this work. We would also like to thank A/P David Fletcher and CFX for their technical support and contributions.

REFERENCES

DALLY, B.B., FLETCHER, D.F. and MASRI, A.R., (1998), "Flow and Mixing Fields of Turbulent Bluff-Body Jets and Flames", *Combust. Theory Modelling*, **2**, 193-219.

KELSO, R.M., (2001), "A Mechanism for Jet Precession in Axisymmetric Sudden Expansions", *14th AFMC*, Adelaide, Australia, 829-832.

LAUNDER, B.E., MORSE, A.P., RODI, W., AND SPALDING, D.B., (1972), "The Prediction of Free Shear Flows – A comparison of Six Turbulence Models", *NASA SP-311*.

LUXTON, R.E., NATHAN, G.J. AND LUMINIS PTY. LTD., (1991), "Controlling the Motion of a Fluid Jet", *USA Letters Patent, No. 5,060,867*.

MANIAS, C., BALENDRA, A. AND RETALLACK D., (1996), "New Combustion Technology for Lime Production", *World Cement*, December.

MCGUIRK, J.J. AND RODI, W., (1979), "The Calculation of Three-Dimensional Turbulent Free Jets", *1st Symp. On Turbulent Shear flows*, editors F. Durst, B.E. Launder, F.W. Schmidt and J.H. Whitelaw, 71-83.

MORSE, A.P., (1977), "Axisymmetric Turbulent Shear Flows with and without Swirl", *Ph.D. Thesis*, London University.

NATHAN, G.J., HILL, S.J. AND LUXTON, R.E., (1998), "An Axisymmetric 'Fluidic' Nozzle to Generate Jet Precession", *J. Fluid Mech.*, **370**, 347-380.

NATHAN, G.J. AND HILL, S.J., (2002), "Full Scale Assessment of the Influence of a Precessing Jet of Air on the Performance of Pulverised Coal Flame in a Cement Kiln", *6th European Conference on Industrial Furnaces and Boilers (INFUB)*, Lisbon, Portugal, April 2-5.

NEWBOLD, G.J.R., (1997), "Mixing and Combustion in Precessing Jet Flows", *Ph.D. Thesis*, The University of Adelaide, Australia.

NOBES, D.S., NEWBOLD, G.J.R., HASSELBRINK, E.F., SU, L., MUNGAL, M.G. AND NATHAN, G.J., (1998), "PIV and PLIF Measurements in Precessing and Round Jets - Report 1": *Measurements and Data, Internal Report*, The University of Adelaide, Australia.

PARHAM, J.J., (1998), "Prediction and Control of Heat Flux and NOx Emissions in Gas Fired Rotary Kilns", *Upgrade Report*, Dept. Mech. Eng., The University of Adelaide, Australia.

PARHAM, J.J., (2000), "Control and Optimisation of Mixing and Combustion from a Precessing Jet Nozzle", *Ph.D. Thesis*, The University of Adelaide, Australia.

POPE, S.B., (1978), "An Explanation of the Round Jet/Plane Jet Anomaly", *AIAA Journal* **16**, 3.

RAPSON, D., STOKES, B. AND HILL, S., (1995), "Kiln Flame Shape Optimisation using a Gyro-Therm Gas Burner", *World Cement*, **26**, 7.

RICHARDS, C.D. AND PITTS, W.M., (1993), "Global Density Effects on the Self-Preservation Behaviour of Turbulent Free Jets", *J. Fluid Mech.*, **254**, 417-435.

SMITH, E.J., NATHAN, G.J. AND DALLY, B.B., (2003), "Assessment of the Robustness of the K-Epsilon Model to Variations in Turbulence Constants for Simulation of Increased Jet Spreading", *EMAC 2003 Proceedings*, editors R.L. May and W.F. Blyth.

WONG, C.Y., NATHAN, G.J. AND O'DOHERTY, T., (2002), "The Effect of Different Initial Conditions on the Exit Flow from a Fluidic Precessing Jet Nozzle", *11th International Symposium on Applications of Laser Techniques to Fluid Mechanics*, Lisbon, 8-11 July.